IEEE Access
Multidisciplinary | Rapid Review | Open Access Journal

Received 1 January 2023, accepted 19 February 2023, date of publication 28 February 2023, date of current version 24 March 2023.

Digital Object Identifier 10.1109/ACCESS.2023.3250253

APPLIED RESEARCH

Application of QR Code for Localization and Navigation of Indoor Mobile Robot

SY-HUNG BACH[1], PHAN-BUI KHOI[2], AND SOO-YEONG YI[1]
[1]Department of Electrical and Information Engineering, Seoul National University of Science and Technology, Seoul 01811, South Korea
[2]School of Mechanical Engineering, Hanoi University of Science and Technology, Hanoi 10000, Vietnam

Corresponding author: Soo-Yeong Yi (suylee@seoultech.ac.kr)

This work was supported by the Research Program by the Seoul National University of Science and Technology.

ABSTRACT Localization is essential for the autonomous navigation of a mobile robot. Because the error of the internal dead-reckoning localization increases with time, the localization error should be corrected periodically using external environmental information. This study presents a practical application of Quick Response (QR) codes to correct the localization error by combining the external QR code information and the internal encoder values. Each QR code contains the information of its own global coordinates and is attached as a one-dimensional array on vertical, thus walls reducing the number of QR codes required for localization. Whenever a QR code is detected and decoded by the mobile robot, the relative transformation between the QR code and the robot can be computed and the pose estimation for the robot is corrected by the extended Kalman filter. Experimental results demonstrate the performance of the localization and autonomous navigation of the mobile robot. The influence of the distance between adjacent QR codes in the environment on the localization performance was also addressed and verified by experiments.

INDEX TERMS Localization, autonomous mobile robot, QR code, artificial landmark, extended kalman filter.

I. INTRODUCTION

There has been increasing attention to mobile robots in factories and warehouses to enhance the level of automation. In order to improve the efficiency and the reliability of the mobile robot, dependable methods of localization and navigation are required for practical purposes. Localization is a process for a mobile robot to obtain its pose (the position and the heading angle) in the environment [1], [2]. For dead-reckoning localization, internal sensors such as the Inertial Measurement Unit (IMU) or the encoders combined with driving motors have been used [3]. However, because the localization error of the dead-reckoning increases with time, it should be corrected periodically by external information about the environment. The external information can be represented by two kinds of characteristic marks: natural features and artificial landmarks.

Walls, corners, or pillars in the environment are the typical natural features and can be detected by ultrasonic, Light Detection and Ranging (LiDAR), or camera sensors. When the features are detected, they are matched with prior sensor information and the pose of the mobile robot can be estimated. In [4], a ground-facing camera is used to detect and match the natural features on the ground. In [5], an omnidirectional camera is adopted to acquire the rich visual features in the environment. A method to combine a Time-of-Flight camera with an IMU is shown in [6]. Much research has been conducted on Simultaneous Localization And Map-building (SLAM), which builds a map of features and performs localization simultaneously by detecting the natural features of the environment [7], [8], [9], [10]. SLAM is an advanced algorithm for localization and has many advantages, but it requires expensive sensors and a large amount of computation. Also, the loop-closure problem of SLAM demands additional batch optimization in general [11], [12], [13]. Therefore, a more efficient and simple localization and navigation method is needed for mobile robots in practical purpose.

On the other hand, distinctive artificial landmarks can be used instead of natural features because they are relatively simple to detect in general. In [14], a set of arranged circles

The associate editor coordinating the review of this manuscript and approving it for publication was Halil Ersin Soken.

This work is licensed under a Creative Commons Attribution-NonCommercial-NoDerivatives 4.0 License.
For more information, see https://creativecommons.org/licenses/by-nc-nd/4.0/

is attached on the ceiling of the environment to guide the direction of mobile robot. Omnidirectional vision and circular landmarks are used to estimate the pose of a mobile robot in [15]. A calibration grid is adopted as an artificial landmark and mounted on a mobile robot for the localization in [16]. In [17], a 2D code is designed as the artificial landmark for real-time navigation of a mobile robot. Visible light communication is adopted as an artificial landmark and attached on the ceiling for the localization in [18]. In the case of using the artificial landmarks, the detection of the landmarks and the localization of a mobile robot can be accomplished effectively with a small amount of computation despite the inconvenience of placing the landmarks in the environment. Quick Response (QR) codes can also be used as the artificial landmark for the localization.

A QR code is a type of matrix code that contains its identification data and user defined data. The QR code system is prevalent in industry due to its rapid and secure readability [19]. For the localization of a mobile robot, a set of QR codes is placed on the ground [20] and on the ceiling [21] of the environment. In such cases, a large number of QR codes is required because they should be placed as a 2D array on the ground or the ceiling. When installing them as above, the vertical distance from the camera to the plane of the QR codes is constant and the image size of the QR code on a camera sensor does not change while the mobile robot is moving [20], [21]. However, because the relative direction of a mobile robot to a QR code can change according to the heading of the mobile robot, the detection and decoding rates of the QR codes deteriorates. Ambient illumination would also interfere the detection of QR code by camera sensor.

This study uses a set of QR codes arranged in a one-dimensional array on a vertical plane such as a wall or pillar in the environment. This reduces the total number of QR codes required for the localization and minimizes the problem of ambient illumination [22]. In the proposed arrangement of QR codes, the distance between the camera on the mobile robot to the plane of the QR code can be changed according to the motion of the mobile robot. In spite of this, it is relatively simple to detect and decode the QR codes by the camera on the mobile robot because they have a fixed height and orientation about the frontal axis. When the camera detects a QR code, the transformation between the QR code and the camera is computed, and the pose of the robot estimated by the extended Kalman filter (EKF) is corrected [23]. The influence of the distance between each QR code on the localization performance of mobile robots has been experimentally verified.

The organization of this paper is as follow: In Section II, the properties of QR codes are briefly described and the transformation between a QR code and a mobile robot is presented. In Section III, a method for estimating the pose of a mobile robot is presented by combining the internal encoder sensor data combined with the external QR code data. In Section IV, the performance of the localization and the influence of the number of QR codes in the environment are demonstrated with experiment results. Concluding remarks are presented in Section V.

II. QR CODE DETECTION

A QR code consists of black squares arranged in a square grid on a white background, which can be detected by an imaging device and decoded to be properly interpreted. A QR code contains position markers, alignment makers, the timing pattern to determine the size of the code, version and format information, and data and error correction keys [24]. There exist many open libraries to generate and detect a QR code. The ZBar library is adopted as it is rapid and suitable for embedded applications.

A set of QR codes containing identification data and its own global coordinates is attached to vertical planes of the mobile robot environment as the artificial landmarks. It is assumed that a mobile robot moves on horizontal ground and the QR codes are aligned with the ground; the QR codes have rotation only about the vertical axis.

When a QR code is detected by the camera, the global coordinates of the mobile robot can be obtained by (1)

$$\mathbf{T}_g^m = \mathbf{T}_g^{QR} \cdot \mathbf{T}_{QR}^{cam} \cdot \mathbf{T}_{cam}^m \tag{1}$$

where $\mathbf{T}_g^m$ is the homogeneous transformation matrix from the global frame to the moving frame of the mobile robot. The matrices $\mathbf{T}_g^{QR}$, $\mathbf{T}_{QR}^{cam}$, and $\mathbf{T}_{cam}^m$ represent the transformation from the global frame to the QR code frame, the transformation from the QR code frame to the camera frame, and the transformation from the camera frame to the frame of the mobile robot, respectively. The transformation matrix, $\mathbf{T}_g^m$, contains the position vector, $\begin{bmatrix} x & y & z & 1 \end{bmatrix}^t$, and the orientation angle, θ, about the vertical z-axis as (2)

$$\mathbf{T}_g^m = \begin{bmatrix} \cos\theta & -\sin\theta & 0 & x \\ \sin\theta & \cos\theta & 0 & y \\ 0 & 0 & 1 & z \\ 0 & 0 & 0 & 1 \end{bmatrix} \tag{2}$$

The relationships between the coordinates are shown in Fig. 1. In order to obtain $\mathbf{T}_g^m$ by (1) with known $\mathbf{T}_g^{QR}$ and $\mathbf{T}_{cam}^m$, it is necessary to measure $\mathbf{T}_{QR}^{cam}$ by a camera in real-time during navigation. The homogeneous transformation matrix, $\mathbf{T}_{QR}^{cam}$, consists of a position vector, $\mathbf{P}_{QR}^{cam}$, and a rotation matrix, $\mathbf{R}_{QR}^{cam}$. In the image coordinates of a QR code, the position vectors of four corners of the QR code can be represented by (3) taking the imaging parameters into consideration.

$$\begin{bmatrix} a_j \\ b_j \\ 1 \end{bmatrix} = \begin{bmatrix} f_x & 0 & c_x & 0 \\ 0 & f_y & c_y & 0 \\ 0 & 0 & 1 & 0 \end{bmatrix} \mathbf{T}_{QR}^{cam} \begin{bmatrix} \mathbf{P}_j \\ 1 \end{bmatrix}, \quad j = 1, \cdots, 4$$

$$\mathbf{T}_{QR}^{cam} = \begin{bmatrix} \mathbf{R}_{QR}^{cam} & \mathbf{P}_{QR}^{cam} \\ 0_{1\times 3} & 1 \end{bmatrix} \tag{3}$$

where $\mathbf{P}_j$ represents the actual 3D position vector of the j^{th} corner of the QR code and $\mathbf{I}_j = \begin{bmatrix} a_j & b_j \end{bmatrix}^t$ denotes the corresponding 2D position vector in the image frame acquired

by camera. It is noted that $\mathbf{P}_j$ is represented in the QR code coordinate frame and is calculated from the actual size of the QR code. In (3), $(f_x,\ f_y)$ and $(c_x,\ c_y)$ are the focal length and the principal point of the camera, respectively.

Fig. 2 shows the relationship between $\mathbf{P}_j$ and $\mathbf{I}_j$. From (3), it is possible to obtain the rotation matrix, $\mathbf{R}_{QR}^{cam}$, and the position vector, $\mathbf{P}_{QR}^{cam}$, of $\mathbf{T}_{QR}^{cam}$ as (4)

$$\begin{bmatrix} \mathbf{R}_{QR}^{cam} & \mathbf{P}_{QR}^{cam} \end{bmatrix}_{3\times4} = \boldsymbol{\lambda}^{-1} \cdot \mathbf{I} \cdot \mathbf{P}^{-1} \tag{4}$$

where $\boldsymbol{\lambda}$ represents the focal lengths and the imaging parameters of a camera as

$$\boldsymbol{\lambda}_{3\times3} = \begin{bmatrix} f_x & 0 & c_x \\ 0 & f_y & c_y \\ 0 & 0 & 1 \end{bmatrix}.$$

The imaging parameters in $\boldsymbol{\lambda}$ can be obtained via preliminary camera calibration. The matrices, $\mathbf{I}_{3\times4}$ and $\mathbf{P}_{4\times4}$ in (4) are augmented by the four corner vectors of the QR code as

$$\mathbf{I}_{3\times4} = \begin{bmatrix} \mathbf{I}_1 & \mathbf{I}_2 & \mathbf{I}_3 & \mathbf{I}_4 \\ 1 & 1 & 1 & 1 \end{bmatrix}, \quad \mathbf{P}_{4\times4} = \begin{bmatrix} \mathbf{P}_1 & \mathbf{P}_2 & \mathbf{P}_3 & \mathbf{P}_4 \\ 1 & 1 & 1 & 1 \end{bmatrix}.$$

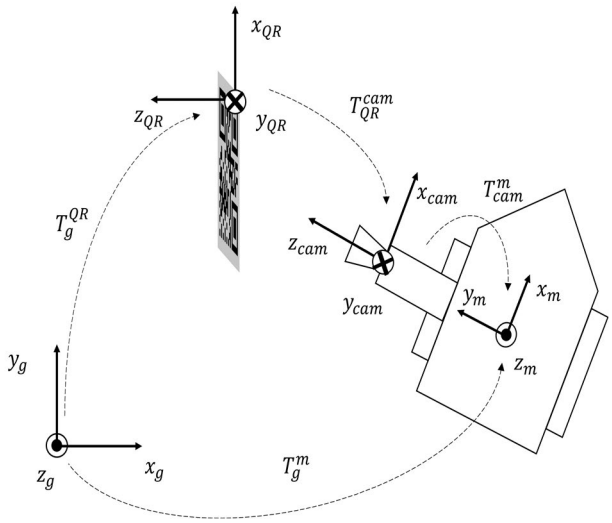

FIGURE 1. Transformation between coordinates.

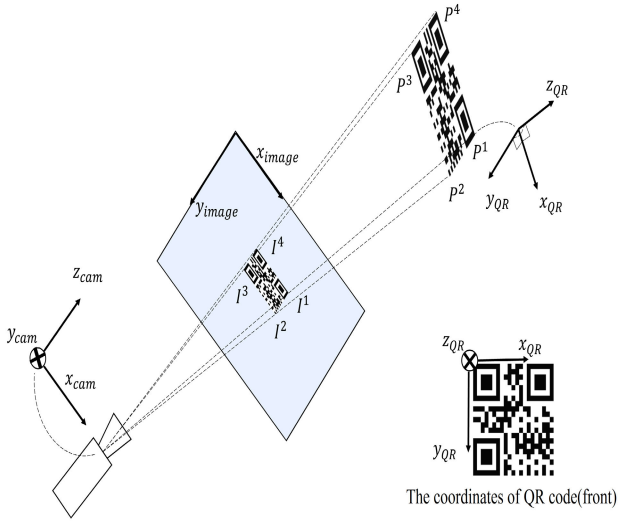

FIGURE 2. Relationship between QR code and camera coordinates.

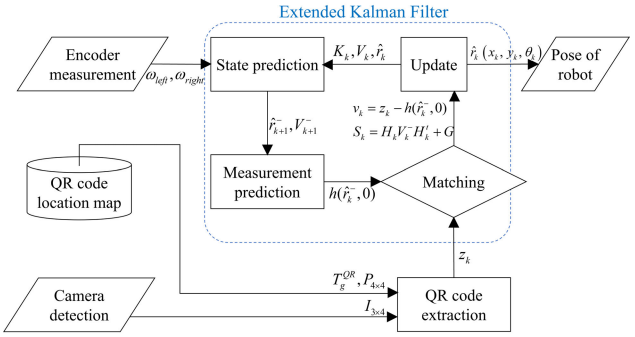

FIGURE 3. Localization using QR codes.

III. LOCALIZATION AND AUTONOMOUS NAVIGATION USING QR CODES

A. EXTENDED KALMAN FILTER FOR LOCALIZATION

Fig. 3 shows the block diagram of the mobile robot localization algorithm presented in this study. While the mobile robot is moving, the pose of the mobile robot is estimated relying on the internal encoder sensors of the driving motors and the accumulated error of the pose estimation can be corrected by combining the internal encoder sensor and the external QR code whenever a QR code is detected. In order to combine the estimation and the correction for the pose of the mobile robot, the EKF is adopted [23].

Referring to Fig. 4, the velocity kinematics of a bi-wheeled mobile is described as follows:

$$\begin{aligned} \mathbf{r}_{k+1} &= \mathbf{f}(\mathbf{r}_k, \mathbf{u}_k, \mathbf{q}_k) \\ &= \begin{bmatrix} x_k + v_k T \cos\left(\theta_k + \dfrac{\omega_k T}{2}\right) + q_{x,k} \\ y_k + v_k T \sin\left(\theta_k + \dfrac{\omega_k T}{2}\right) + q_{y,k} \\ \theta_k + \omega_k T + q_{\theta,k} \end{bmatrix} \end{aligned} \tag{5}$$

where $\mathbf{r}_k = [x_k,\ y_k,\ \theta_k]^t$ represents the pose of the mobile robot, $\mathbf{q}_k = \begin{bmatrix} q_x,\ q_y,\ q_\theta \end{bmatrix}^t$ denotes the state noise vector that is random Gaussian with zero mean and $\mathbf{Q}$ variance, and $(v_k,\ \omega_k)$ denotes the linear and angular velocity commands. The subscript k implies the time index. The size of the mobile robot is represented by the distance, L, between two wheels and the radius of wheel, R. In (5), T denotes the sampling interval.

The localization algorithm using the EKF is described as follows:

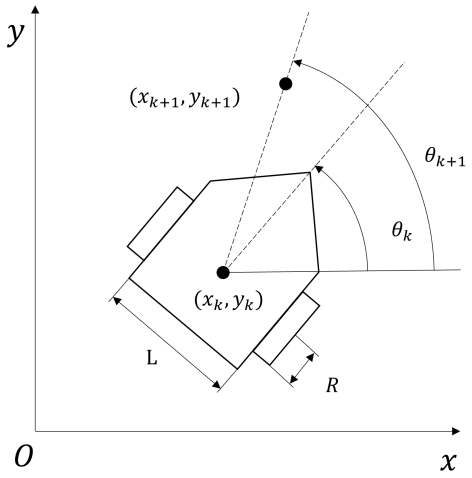

FIGURE 4. The kinematics parameters of a bi-wheeled mobile robot.

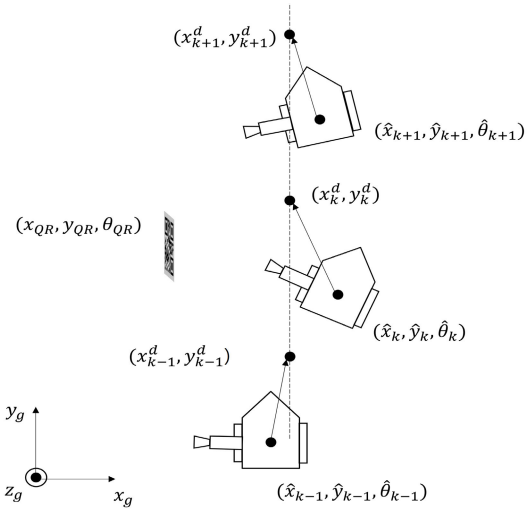

FIGURE 5. The navigation of a mobile robot.

■ **Prediction**: A priori estimation, $\hat{\mathbf{r}}_k^-$ for $\mathbf{r}_k$ is given by (6).

$$\hat{\mathbf{r}}_{k+1}^- = \begin{bmatrix} \hat{x}_k + v_k T \cos\left(\hat{\theta}_k + \dfrac{\omega_k T}{2}\right) \\ \hat{y}_k + v_k T \sin\left(\hat{\theta}_k + \dfrac{\omega_k T}{2}\right) \\ \hat{\theta}_k + \omega_k T \end{bmatrix} = \mathbf{f}\left(\hat{\mathbf{r}}_k, \mathbf{u}_k, 0\right) \tag{6}$$

$$\mathbf{V}_{k+1}^- = \mathbf{A}_k \mathbf{V}_k \mathbf{A}_k^t + \mathbf{Q} \tag{7}$$

where

$$\mathbf{A}_k = \frac{\partial\, \mathbf{f}\left(\hat{\mathbf{r}}_k, \mathbf{u}_k, 0\right)}{\partial\, \mathbf{r_k}} = \begin{bmatrix} 1 & 0 & -v_k T \sin\left(\hat{\theta}_k + \dfrac{\omega_k T}{2}\right) \\ 0 & 1 & v_k T \cos\left(\hat{\theta}_k + \dfrac{\omega_k T}{2}\right) \\ 0 & 0 & 1 \end{bmatrix} \tag{8}$$

In (7), $\mathbf{V}_{k+1}^-$ and $\mathbf{V}_k$ represent the *priori* and *posteriori* error covariance matrices.

■ **Correction:** The priori estimation, $\hat{\mathbf{r}}_k^-$, is corrected by the QR code measurement resulting in a posteriori estimation, $\hat{\mathbf{r}}_k$, as follows:

$$\mathbf{K}_k = \mathbf{V}_k^- \mathbf{H}_k^t \left(\mathbf{H}_k \mathbf{V}_k^- \mathbf{H}_k^t + \mathbf{G}\right)^{-1} \tag{9}$$

$$\mathbf{V}_k = \left(\mathbf{I} - \mathbf{K}_k \mathbf{H}_k\right) \mathbf{V}_k^- \tag{10}$$

$$\hat{\mathbf{r}}_k = \hat{\mathbf{r}}_k^- + \mathbf{K}_k \left\{\mathbf{z}_k - h\left(\hat{\mathbf{r}}_k^-, 0\right)\right\} \tag{11}$$

$$\mathbf{z}_k = h\left(\mathbf{r}_k, \mathbf{g}_k\right) = \begin{bmatrix} x_k + g_{x,k} \\ y_k + g_{y,k} \\ \theta_k + g_{\theta,k} \end{bmatrix} = \begin{bmatrix} x_{\mathbf{T}_g^m} + g_{x,k} \\ y_{\mathbf{T}_g^m} + g_{y,k} \\ \theta_{\mathbf{T}_g^m} + g_{\theta,k} \end{bmatrix} \tag{12}$$

where $(x_{T_g^m},\ y_{T_g^m},\ \theta_{T_g^m})$ comes from the measurement of a QR code at k as described in Section II and $\mathbf{g}_k = \left[g_{x,k},\ g_{y,k},\ g_{\theta,k}\right]^t$ represents the noise in the measurement that is Gaussian random noise with zero mean and $\mathbf{G}$ covariance.

The variances of $\mathbf{Q}$ and $\mathbf{G}$ are estimated by simulations and experiments. The Jacobian matrix, $\mathbf{H}_k$, is described as follows:

$$\mathbf{H}_k = \frac{\partial h}{\partial \mathbf{r}_k}\left(\hat{\mathbf{r}}_k, 0\right) = \begin{bmatrix} 1 & 0 & 0 \\ 0 & 1 & 0 \\ 0 & 0 & 1 \end{bmatrix} \tag{13}$$

Herein, the loosely coupled method is used for the sensor fusion [25].

B. AUTONOMOUS NAVIGATION BASED ON LOCALIZATION

A tracking control for the desired trajectory of a mobile robot is shown in Fig. 5. The linear and angular velocity commands are given by:

$$\begin{aligned} v_k &= \frac{K_v}{T}\sqrt{\left(x_k^d - \hat{x}_k\right)^2 + \left(y_k^d - \hat{y}_k\right)^2} \\ \omega_k &= \frac{K_\omega}{T}\left\{\tan^{-1}\left(\frac{y_k^d - \hat{y}_k}{x_k^d - \hat{x}_k}\right) - \hat{\theta}_k\right\} \end{aligned} \tag{14}$$

where $(x^d,\ y^d,\ \theta^d)$ denotes the desired trajectory and $(\hat{x},\ \hat{y},\ \hat{\theta})$ is the estimated pose of the mobile robot from the EKF. In (14), K_v and K_ω are the control gains of the linear velocity command and the angular velocity command, respectively.

IV. RESULTS OF EXPERIMENTS

In order to verify the proposed method of the localization and autonomous navigation, experiments were conducted using a bi-wheeled mobile robot. The experiment environments and the mobile robot are shown in Fig. 6. A set of QR codes is attached to the walls of the environment with intervals of about 1 m. The size of the QR codes is 10 cm × 10 cm and the mobile robot has two cameras on the left and right sides to detect them. The detectable range of a QR code by camera using the ZBar library is within 20 cm to 80 cm. Every via point on the desired trajectory is within this range.

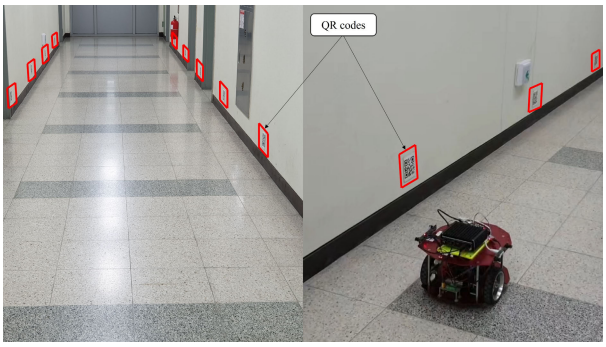

FIGURE 6. Mobile robot environment.

The sampling time for the trajectory tracking control, T, is 50 ms. The blueprint of the building was used as a map for the mobile robot environment. This map was used to select known locations to set up the QR codes. The values of variances of $\mathbf{Q}$ and $\mathbf{G}$ used in these experiments were $\mathbf{Q} = diag(0.95)$ and $\mathbf{G} = diag(0.001)$, respectively.

A. EXPERIMENT IN ENVIRONMENT 1

The results of the first experiment are shown in Fig. 7 and Fig. 8. The total length of the path in this experiment is around 40.5 m; the distance between adjacent QR codes, d_{QR}, is around 1 m and the number of QR codes, n_{QR}, is 32. Fig. 7 shows the localization using only the internal encoder sensor (dash-dot green line) and the localization using both the encoder and the QR code with the EKF (solid blue line). The red line represents the desire trajectory. As shown in the figure, the estimated trajectory using only the encoder sensor has a large error from the desired trajectory. Comparatively, in the case of the pose estimation combining the encoder and the QR codes, the cumulative localization error is reset

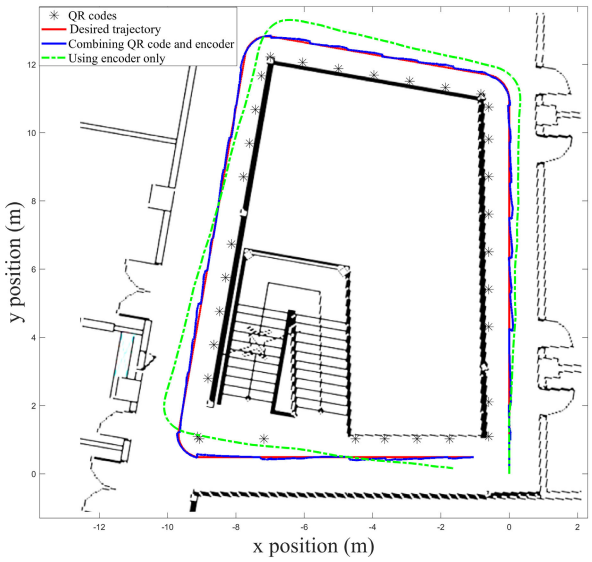

FIGURE 7. Localization results from the experiment in environment 1.

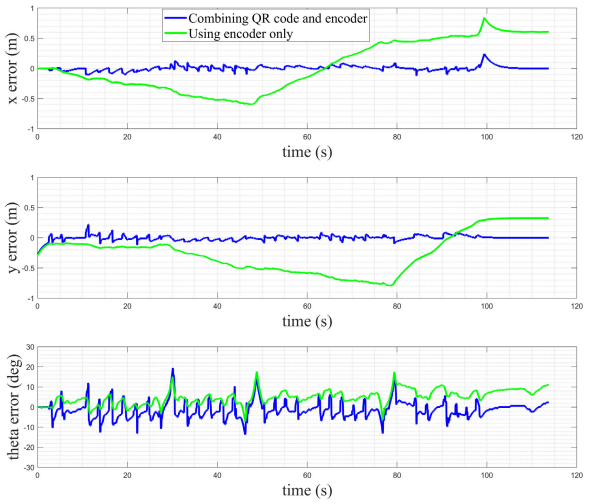

FIGURE 8. Localization error from the experiment in environment 1.

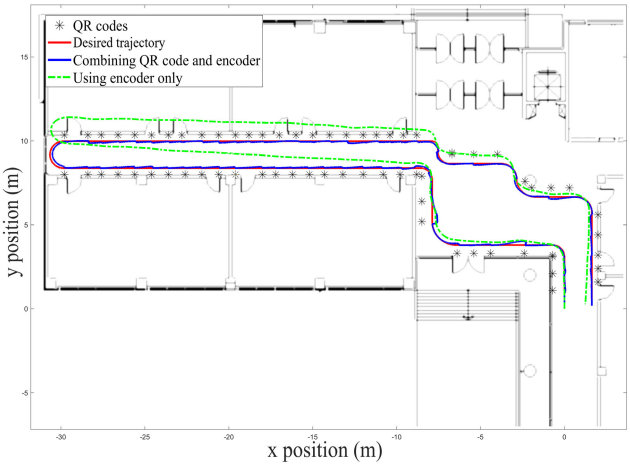

FIGURE 9. Localization results from the experiment in environment 2.

whenever a QR code is detected. The tracking errors in the experiment are shown in Fig. 8.

B. EXPERIMENT IN ENVIRONMENT 2

Figs. 9 and 10 show the results of the second experiment. In this experiment, the length of the path is around 64.6 m, the distance between adjacent QR codes is $d_{QR} = 1$m, and the number of QR codes is $n_{QR} = 68$. Fig. 9 shows the localization using only the internal encoder (dash-dot green line) and the localization using both the encoder and the QR code with the EKF (solid blue line). The tracking errors of the experiment are shown in Fig. 10.

C. EXPERIMENTS ON LOCALIZATION PERFORMANCE ACCORDING TO DISTANCE BETWEEN QR CODES

In order to investigate the effect of distance between the adjacent QR codes, d_{QR} on the localization performance, additional experiments were conducted by changing d_{QR}, to 1 m, 2 m, and 4 m in the same environments of experiments 1 and 2 above as shown in Table 1. Because the accumulated

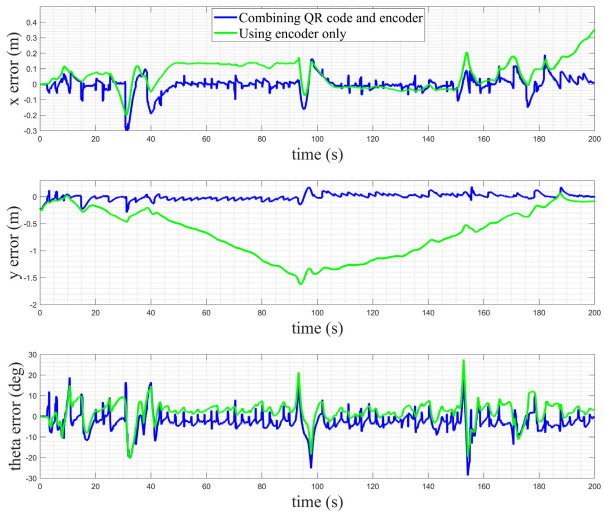

FIGURE 10. Localization error from the experiment in environment 2.

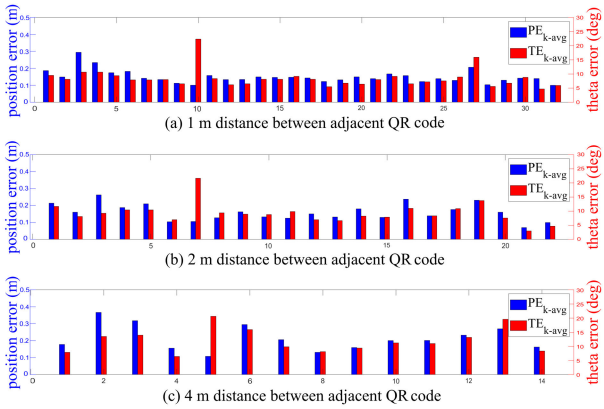

FIGURE 11. PE_{k-avg} and TE_{k-avg} according to distance between adjacent QR codes in the experiment of environment 1.

dead-reckoning localization error is eliminated periodically at the instant of QR code detection in the localization algorithm, it is expected that the pose estimation error is the largest right before that instant. Thus, the localization performance is evaluated as the deviation between the predicted pose of the mobile robot in (6) and the measured pose in (4) at every instant of QR code detection while tracking the desired trajectory. This experiment was carried out five times for reliability of the performance investigation. The localization performance index is represented as (15).

$$\begin{aligned} PE_{tot-avg} &= \sum_k PE_{k-avg} \\ &= \sum_k \left\{ \frac{1}{N} \sum_n \sqrt{(\hat{x}_k^- - x_k)^2 + (\hat{y}_k^- - y_k)^2} \right\} \\ TE_{tot-avg} &= \sum_k TE_{k-avg} = \sum_k \left\{ \frac{1}{N} \sum_n \left| \hat{\theta}_k^- - \theta_k \right| \right\} \end{aligned} \quad (15)$$

where $N = 5$ is the number of experiments and k denotes the time instant of detecting a QR code. Fig. 11 shows PE_{k-avg} and TE_{k-avg} among the five experiments in the vicinity of every QR code from the experiment in *Environment 1*. It is obvious that the localization errors increase according to the distance of the adjacent QR code. Therefore, the distance between the adjacent QR codes should be determined by taking into account the trajectory tracking accuracy.

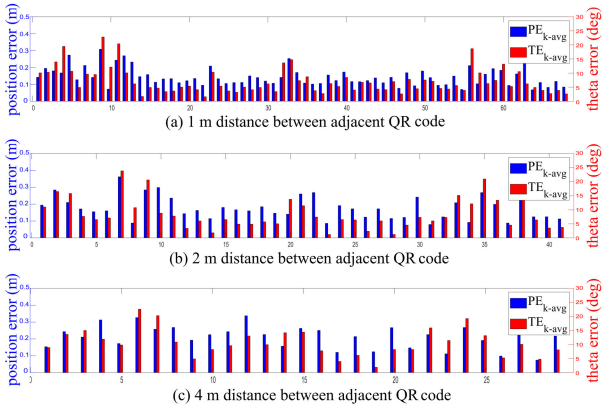

FIGURE 12. PE_{k-avg} and TE_{k-avg} according to distance between adjacent QR codes in the experiment of environment 2.

TABLE 1. The effect Of QR code density on localization performance.

	d_{QR}	n_{QR}	$PE_{tot-avg}$		$TE_{tot-avg}$	
Env. 1	1 m	32	0.150	100%	8.426	100%
	2 m	22	0.159	106%	9.303	110%
	4 m	14	0.213	142%	12.081	143%
Env. 2	1 m	68	0.145	100%	7.187	100%
	2 m	41	0.181	125%	8.614	120%
	4 m	29	0.214	148%	10.764	150%

Similar results are obtained from the experiment in *Environment 2* as shown in Fig. 12.

The numerical data of the localization performance is summarized in Table 1, where the percent error is presented with respect to the error of $d_{QR} = 1$ m. Table 1 shows that the localization errors increase according to the distance of the adjacent QR codes. It is shown that the errors increase by around 20% in the case of $d_{QR} = 2$ m compared to $d_{QR} = 1$ m. When $d_{QR} = 4$ m, the errors increase by around 50%.

V. CONCLUSION

For a practical application of a mobile robot in industry, a simple and efficient localization method is needed. Because the internal dead-reckoning localization accumulates error over time, the localization error should be corrected periodically using external information from the environment.

The QR code has proven detection and decoding capability and can be used as an external landmark for mobile robot localization. This study presents an application of the QR code for the localization and autonomous navigation of an indoor mobile robot. The accumulated dead-reckoning error is eliminated when a QR code is detected during navigation. The EKF is adopted to combine the internal encoder sensor data and the external QR code information.

Because external QR codes are attached on the vertical plane of the environment, the camera on a mobile robot has relatively small difference in orientation from the QR code, and the ambient illumination has less interference on the image acquisition of the camera, resulting in improved detection rate of the QR code. Performance of the localization is analyzed according to the distance of adjacent QR codes used in the environment, which gives guidance to the number of QR codes to be used. Experimental results show that the positioning error increases by 20% and 50% respectively when d_{QR} is 2 m and 4 m, compared to when $d_{QR} = 1$ m.

ACKNOWLEDGMENT

The support from the Research Program funded by the Seoul National University of Science and Technology is dutifully acknowledged. The authors would like to thank Gwa-Cheol Jeong for his help in the experiments.

REFERENCES

[1] R. Siegwart, I. R. Nourbakhsh, and D. Scaramuzza, *Introduction to Autonomous Mobile Robots*. Cambridge, MA, USA: MIT Press, 2011.
[2] S. Huang and G. Dissanayake, "Robot localization: An introduction," in *Wiley Encyclopedia of Electrical and Electronics Engineering*. New York, NY, USA: Wiley, 1999.
[3] B.-S. Cho, W.-S. Moon, W.-J. Seo, and K.-R. Baek, "A dead reckoning localization system for mobile robots using inertial sensors and wheel revolution encoding," *J. Mech. Sci. Technol.*, vol. 25, no. 11, pp. 2907–2917, Nov. 2011.
[4] G. Panahandeh and M. Jansson, "Vision-aided inertial navigation based on ground plane feature detection," *IEEE/ASME Trans. Mechatronics*, vol. 19, no. 4, pp. 1206–1215, Aug. 2014.
[5] T. Goedeme, T. Tuytelaars, L. Van Gool, G. Vanacker, and M. Nuttin, "Feature based omnidirectional sparse visual path following," in *Proc. IEEE/RSJ Int. Conf. Intell. Robots Syst.*, Aug. 2005, pp. 1806–1811.
[6] M. Yekkehfallah, M. Yang, Z. Cai, L. Li, and C. Wang, "Accurate 3D localization using RGB-TOF camera and IMU for industrial mobile robots," *Robotica*, vol. 39, no. 10, pp. 1816–1833, Oct. 2021.
[7] F. Fraundorfer, C. Engels, and D. Nister, "Topological mapping, localization and navigation using image collections," in *Proc. IEEE/RSJ Int. Conf. Intell. Robots Syst.*, Oct. 2007, pp. 3872–3877.
[8] C. Lee and D. Kim, "Visual homing navigation with Haar-like features in the snapshot," *IEEE Access*, vol. 6, pp. 33666–33681, 2018.
[9] Y. Jia, X. Yan, and Y. Xu, "A survey of simultaneous localization and mapping for robot," in *Proc. IEEE 4th Adv. Inf. Technol., Electron. Autom. Control Conf. (IAEAC)*, Dec. 2019, pp. 857–861.
[10] S.-H. Park and S.-Y. Yi, "Least-square matching for mobile robot SLAM based on line-segment model," *Int. J. Control, Autom. Syst.*, vol. 17, no. 11, pp. 2961–2968, Nov. 2019.
[11] S. Huang, "A review of optimisation strategies used in simultaneous localisation and mapping," *J. Control Decis.*, vol. 6, no. 1, pp. 61–74, Jan. 2019.
[12] C. Chiu and S. Sastry, "Simultaneous localization and mapping: A rapprochement of filtering and optimization-based approaches," EECS Dept. Univ. California, Berkeley, CA, USA, Tech. Rep., UCB/EECS-2021-76, May 2021.
[13] B. Xu, P. Wang, Y. He, Y. Chen, Y. Chen, and M. Zhou, "Leveraging structural information to improve point line visual-inertial odometry," *IEEE Robot. Autom. Lett.*, vol. 7, no. 2, pp. 3483–3490, Apr. 2022.
[14] A. Rusdinar, J. Kim, J. Lee, and S. Kim, "Implementation of real-time positioning system using extended Kalman filter and artificial landmark on ceiling," *J. Mech. Sci. Technol.*, vol. 26, no. 3, pp. 949–958, Mar. 2012.
[15] C.-J. Wu and W.-H. Tsai, "Location estimation for indoor autonomous vehicle navigation by omni-directional vision using circular landmarks on ceilings," *Robot. Auto. Syst.*, vol. 57, no. 5, pp. 546–555, May 2009.
[16] I. Loevsky and I. Shimshoni, "Reliable and efficient landmark-based localization for mobile robots," *Robot. Auto. Syst.*, vol. 58, no. 5, pp. 520–528, May 2010.
[17] B. Dzodzo, L. Han, X. Chen, H. Qian, and Y. Xu, "Realtime 2D code based localization for indoor robot navigation," in *Proc. IEEE Int. Conf.*, Dec. 2013, pp. 486–492.
[18] Q. Liang and M. Liu, "A tightly coupled VLC-inertial localization system by EKF," *IEEE Robot. Autom. Lett.*, vol. 5, no. 2, pp. 3129–3136, Apr. 2020.
[19] C. Aktas, *The Evolution and Emergence of QR Codes*. Newcastle Upon Tyne, U.K.: Cambridge Scholars Publishing, 2017.
[20] P. Nazemzadeh, D. Fontanelli, D. Macii, and L. Palopoli, "Indoor localization of mobile robots through QR code detection and dead reckoning data fusion," *IEEE/ASME Trans. Mechatronics*, vol. 22, no. 6, pp. 2588–2599, Dec. 2017.
[21] H. Zhang, C. Zhang, W. Yang, and C.-Y. Chen, "Localization and navigation using QR code for mobile robot in indoor environment," in *Proc. IEEE Int. Conf. Robot. Biomimetics (ROBIO)*, Dec. 2015, pp. 2501–2506.
[22] R. Couto, J. Leal, P. M. Costa, and T. Galvao, "Exploring ticketing approaches using mobile technologies: QR codes, NFC and BLE," in *Proc. IEEE 18th Int. Conf. Intell. Transp. Syst.*, Sep. 2015, pp. 7–12.
[23] W. Burgard, C. Stachniss, M. Bennewitz, G. Grisetti, and K. Arras, *Introduction to mobile robotic EKF localization*. Breisgau, Germany: Univ. Freiburg, 2010.
[24] T. Soon, "QR code," *Synth. J.*, pp. 59–78, 2008.
[25] S. Y. Kim, K. S. Yoon, D. H. Lee, and M. H. Lee, "The localization of a mobile robot using a pseudolite ultrasonic system and a dead reckoning integrated system," *Int. J. Control, Autom. Syst.*, vol. 9, no. 2, pp. 339–347, Apr. 2011.

SY-HUNG BACH received the Mechatronic Engineering degree from the Hanoi University of Science and Technology, in 2020. He is currently pursuing the Ph.D. degree with the Department of Electrical and Information Engineering, Seoul National University of Science and Technology, Seoul, South Korea. His primary research interests include intelligent robots, motion control, cable-driven robots, and walking robots.

PHAN-BUI KHOI received the Doctoral degree in robotics from the Mechanical Engineering Research Institute, Russian Academy of Sciences, in 1997. He is currently an Associate Professor of dynamics and control of robot and mechatronic system with the Hanoi University of Science and Technology. His current research interests include robots applying in mechanical engineering and service, dynamics of serial, parallel and cooperate robots, force control, fuzzy control, control of robots, and mechatronic systems, based on artificial intelligence, hedge algebras, and genetic algorithm.

SOO-YEONG YI received the M.S. and Ph.D. degrees in electrical engineering from the Korea Advanced Institute of Science and Technology, in 1990 and 1994, respectively. From 1995 to 1999, he was with the Human Robot Research Center, Korea Institute of Science and Technology, as a Senior Researcher. He was a Professor with the Division of Electronics and Information Engineering, Chonbuk National University, South Korea, from September 1999 to February 2007. He was also a Postdoctoral Researcher with the Department of Computer Science, University of Southern California, Los Angeles, in 1997, and a Visiting Researcher with the Department of Electrical and Computer Engineering, University of Illinois at Urbana–Champaign, in 2005. He is currently with the Department of Electrical and Information Engineering, Seoul National University of Science and Technology, South Korea. His primary research interests include robot vision and intelligent control theory.